Tribology Letters (2020) 68:41
https://doi.org/10.1007/s11249-020-1286-0

ORIGINAL PAPER

# In-Situ Formation of $MoS_2$ and $WS_2$ Tribofilms by the Synergy Between Transition Metal Oxide Nanoparticles and Sulphur-Containing Oil Additives

**Manel Rodríguez Ripoll**[1] · **Agnieszka Maria Tomala**[1,2] · **Luka Pirker**[3] · **Maja Remškar**[3]

Received: 28 May 2019 / Accepted: 4 February 2020 / Published online: 13 February 2020


**Abstract**
This works investigates the in-situ formation of $MoS_2$ and $WS_2$ tribofilms by the synergy between transition metal oxide nanoparticles and conventional sulphur-containing anti-wear and extreme pressure additives. The formation of these low friction tribofilms can be obtained under reciprocating sliding contact and under extreme pressure conditions, as evidenced using X-ray photoelectron spectroscopy. Under reciprocating sliding conditions, the synergy between transition metal oxide nanoparticles and the ZDDP leads to coefficients of friction around 0.06 before they rise as consequence of oxidation. The synergy is more outstanding in extreme pressure conditions, particularly for $MoO_3$ nanotubes combined with extreme pressure additive. This combination outperforms base oil mixtures containing EP additive or $MoS_2$ nanotubes. While $MoS_2$ nanotubes build superb extreme pressure tribofilms containing iron and molybdenum oxides and sulphides, $MoO_3$ nanotubes are able to build similar tribofilms that can continuously re-sulphurize in the presence of the extreme pressure additive. Despite having a similar chemistry, $MoO_3$ nanotubes are observed to sulphurize more easily when compared to $WO_3$ nanoparticles. The work highlights the tribological potential of these nanoparticles otherwise typically used as precursors for the synthesis of transition metal dichalcogenide nanoparticles.

**Keywords** Nanoparticles · ZDDP · EP · Sulphurization · $MoS_2$ · $WS_2$

## 1 Introduction

The use of transition metal dichalcogenides (TMD) nanoparticles has attracted a great deal of attention in tribology due to their superb frictional performance. The reason for the excellent tribological performance of TMD nanoparticles lies in their layered structure. Some transition metal dichalcogenides ($MS_2$ and $MSe_2$ with M = Mo or W) have a 2D layered structure, characterized by transition metal atoms sandwiched between two layers of chalcogen atoms forming a S–M–S molecular layer [1]. The easy glide between molecular layers provides them with excellent frictional properties [2]. In 1992 and 1993, these 2D materials were firstly synthesized as inorganic fullerene nanoparticles [3, 4]. Soon after, their potential as lubricant additives was envisaged [2] and other morphologies [5] were successfully synthesized. Since then, a vast amount of work has shown their superb frictional and wear performance for lubricating steel contacts and coatings under several contact conditions [6–10]. A large effort has been also devoted for understanding the lubrication mechanism of TMD nanoparticles. Nowadays, it is widely agreed that the main friction reduction mechanism relies on the a gradual exfoliation of layered platelets from the nanoparticles, which adhered to the counter body and enable coefficients of friction around 0.05 [11]. According to some authors, at low contact pressures, rolling of the nanoparticles could still contribute to reduce friction [12]. Particularly interesting is the friction reducing mechanism of TMD nanoparticles at extreme contact pressures. Under severe pressure and temperature conditions, TMD nanoparticles react with iron substrates producing a tribofilm containing iron sulphides and oxides, besides transition metal oxides and dichalcogenides [8], which provides excellent low friction and anti-wear properties.

✉ Manel Rodríguez Ripoll
ripoll@ac2t.at

1 AC2T research GmbH, Wiener Neustadt, Austria

2 Institute for Sustainable Technologies, Radom, Poland

3 Institute Jožef Stefan, Ljubljana, Slovenia

More recently, the interaction of TMD nanoparticles with accompanying lubricant additives has started gathering attention. The reason is that TMD nanoparticles alone are not able to accomplish all roles expected for a lubricant additive, as for instance corrosion or sludge control. Under reciprocating sliding, TMD nanoparticles do show synergy with anti-wear additive ZDDP [9, 13, 14], since layer platelets are able to exfoliate on top of well-formed ZDDP tribofilms. The synergy or antagonism between TMD nanoparticles and co-additives depends in general, on the contact conditions [15, 16]. For instance, whereas TMD nanoparticles and succinimide dispersants have been reported to have antagonistic effects under reciprocating sliding [15, 17], under extreme pressure conditions, the interaction between TMD nanoparticles and succinimide results in the tribochemical formation of TM-sulphide compounds that prevent metal-to-metal contact and increases the load-carrying capacity of the nanolubricant [15]. Under extreme pressure conditions, also the synergy with extreme pressure additives is superb [15]. As mentioned above, TMD nanoparticles partly react with the substrate under EP conditions and build a tribofilm that contains sulphides and $MO_3$ (with M being Mo or W) [8, 15, 18]. The presence of sulphur-containing EP additive allows the in-situ re-sulphurization of the tribofilm during the contact, which results in an improved lubrication performance.

This in-situ re-sulphurization of the oxidized tribofilm can be exploited for the potential use of transition metal oxide nanoparticles in tribological applications. Transition metal oxide compounds such as $MO_3$, $Mo_6S_xI_y$, or $WO_x$–$W_{18}O_{49}$ are typically used as precursors for the synthesis of TMD nanoparticles by high temperature sulphurization in the presence of $H_2S$ or a similar sulphur compound [10, 19–24]. The energy required for the sulphurization of transition metal precursors requires the use of high temperature and/or pressure. However, the high shear occurring at interacting asperities in tribological contacts [25] could be exploited as energy source for sulphurization, thus allowing to skip the sulphurization process of transition metal oxide precursors. Beside the high shears, this approach requires the simultaneous presence of transition metal oxide nanoparticles and sulphur compounds in the lubricant formulation. Sulphur is present in most of the commercially available lubricants nowadays, since they contain anti-wear additives such as zinc dialkyl dithiophosphate (ZDDP) or extreme pressure additives, such as sulphurized olefins [26]. The in-situ sulphurization of $MoO_3$ nanotubes under several contact conditions in the presence of S-containing additives was recently reported [27].

The aim of this paper is to report on a detailed and comparable study of the in-situ sulphurization of selected $MoO_3$ and $WO_3$ nanomaterials in the presence of conventional sulphur-containing lubricant additives such as ZDDP anti-wear additive and sulphurized olefin extreme pressure additive. The approach is verified giving special emphasis to the role of the additive chemistry and contact conditions. The results show an exceptional performance in terms of friction and wear, thus proving that, for friction reduction applications, the sulphurization of transition metal oxide nanoparticles during the synthesis process might be superfluous by utilizing the present approach.

## 2 Experimental

### 2.1 Synthesis and Characterization of Transition Metal Oxide Nanoparticles

The $MoO_3$ nanotubes were synthesized at the Jožef Stefan Institute (Slovenia), whereas the $WO_3$ nanoparticles were commercially available (Sigma-Aldrich, USA). The morphology and crystal structure of both nanomaterials were analysed by scanning electron microscopy (Helios NanoLab 650 FIB-SEM) and transmission electron microscopy (ARM 200 CF-Jeol). The crystal structure of the nanomaterials was examined by XRD at room temperature with D4 Endeavor diffractometer (Bruker AXS) using a quartz monochromatic Cu K$\alpha$1 radiation source ($\lambda = 0.1541$ nm) and a Sol-X dispersive detector.

The $MoO_3$ nanotubes were synthesized using $Mo_6S_2I_8$ nanowires as precursors. The $Mo_6S_2I_8$ nanowires were obtained using stoichiometric amounts of molybdenum (Aldrich 99.9%), sulphur (Aldrich 99%) and iodine (Sigma-Aldrich reagent-plus grade) in evacuated and sealed silica ampoules at 736 °C using a temperature gradient of 5.5 K/cm. The synthesis process let to the formation of $Mo_6S_2I_8$ nanowires with a length of 5 µm and a diameter ranging from 100 to 200 nm [28]. Afterwards, the obtained nanowires were oxidized for 25 h in ambient air at 573 K. The oxidation process results in the formation of polycrystalline $MoO_{3-x}$ nanowires and nanotubes arranged in hedgehog-like self-assemblies (Fig. 1a, b). A thorough characterization of the $MoO_3$ nanotubes is given elsewhere [29]. The nanotube walls are well crystallized and XRD confirms a pure orthorhombic $\alpha$-phase of $MoO_3$ (JCPDS No. 05–0508) (Fig. 2b).

The purchased $WO_3$ nanoparticles were agglomerated into spherical agglomerates with diameters up to several tens of micrometres, as observed in the SEM image (Fig. 1c). Single nanoparticles had a disc shape with wideness up to 100 nm and 20–30 nm thick (Fig. 1d). The TEM image showed a small group of weakly bond $WO_3$ nanoparticles (Fig. 2c), which were single crystalline (Fig. 2d). Distance between the lines corresponding to (002) planes was $3.9 \pm 0.05$ Å. The diffraction pattern (Fig. 2e) and XRD diffraction (Fig. 3f) revealed that $WO_3$ was present in the monoclinic $WO_3$ phase (JCPDS no. 83–0950).

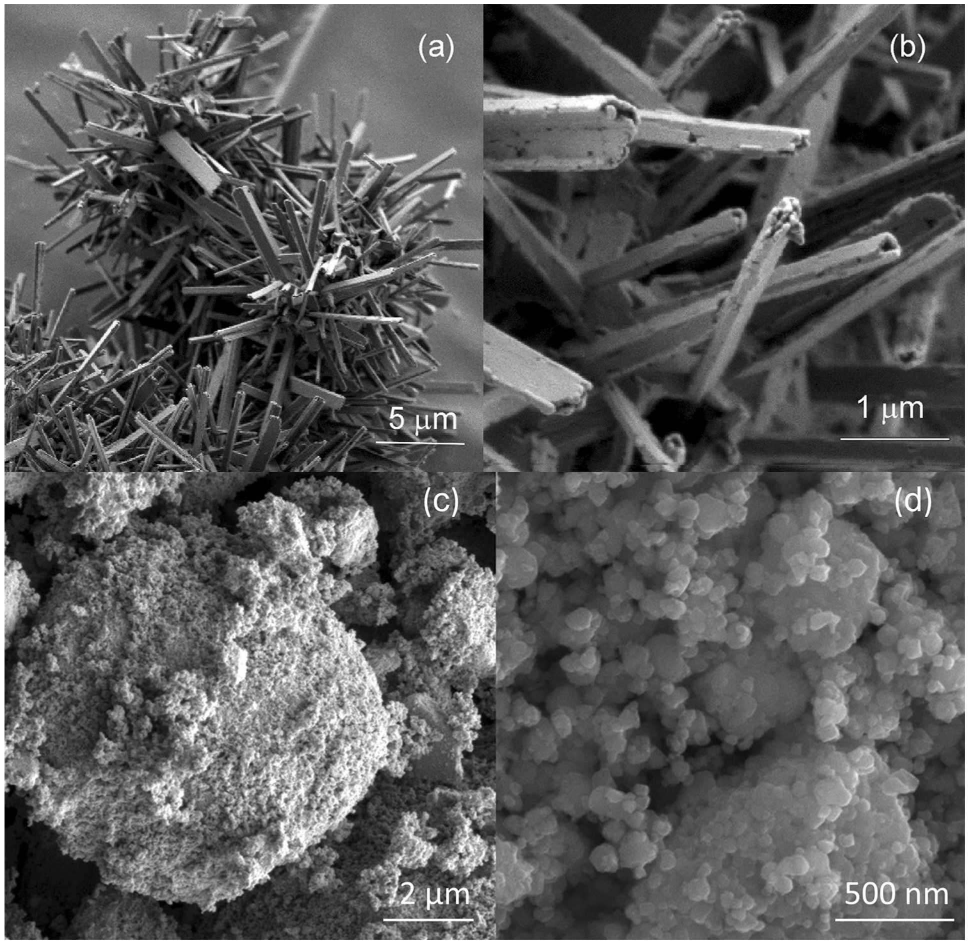


**Fig. 1** SEM micrographs: **a** Hedgehog-like self-assemblies of $MoO_3$ nanowires and nanotubes; **b** Faceted $MoO_3$ nanotubes with a high degree of porosity; **c** globular agglomerates of $WO_3$ nanoparticles with diameters up to a few tens of micrometres; **d** single $WO_3$ nanoparticles with sizes up to 100 nm

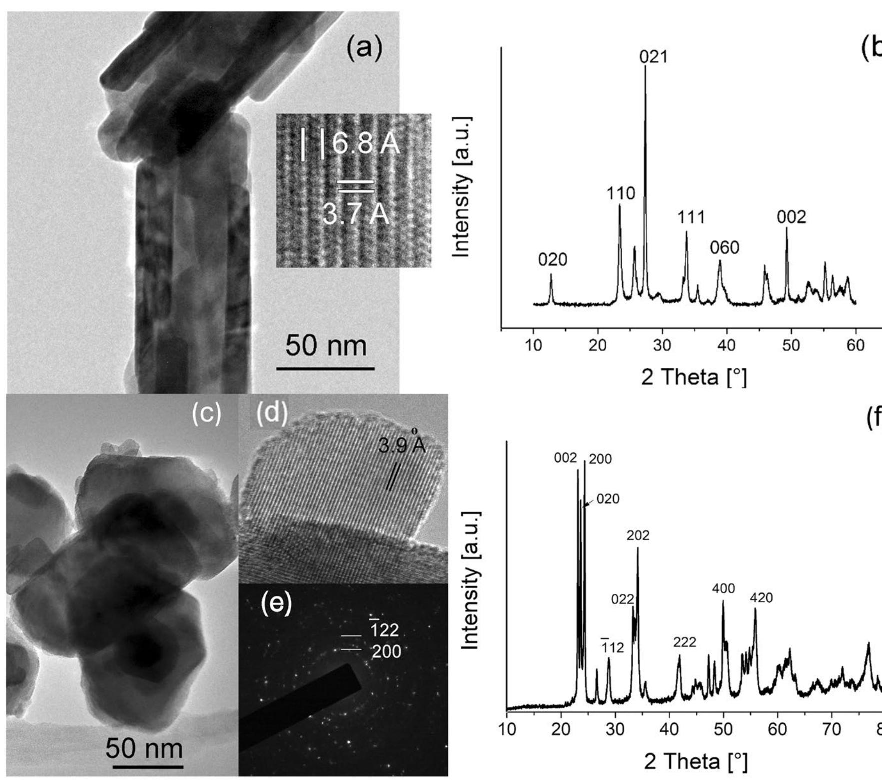


**Fig. 2** TEM images: **a** Polycrystalline structure of $MoO_3$ nanotubes growing along [001] direction with high-resolution image of the nanotube's wall; **b** XRD pattern with some peaks assigned according to the $\alpha$-$MoO_3$ (JCPDS No. 05-0508); **c** Weakly bond group of $WO_3$ nanoparticles; **d** HR-TEM image of a single $WO_3$ nanoparticle revealing the (002) crystal planes; **e** Electron diffraction pattern in accordance with the monoclinic $WO_3$ phase (JCPDF 83-0950); **f** XRD spectrum of $WO_3$ particles indexed in accordance with the monoclinic phase (JCPDF 83-0950)

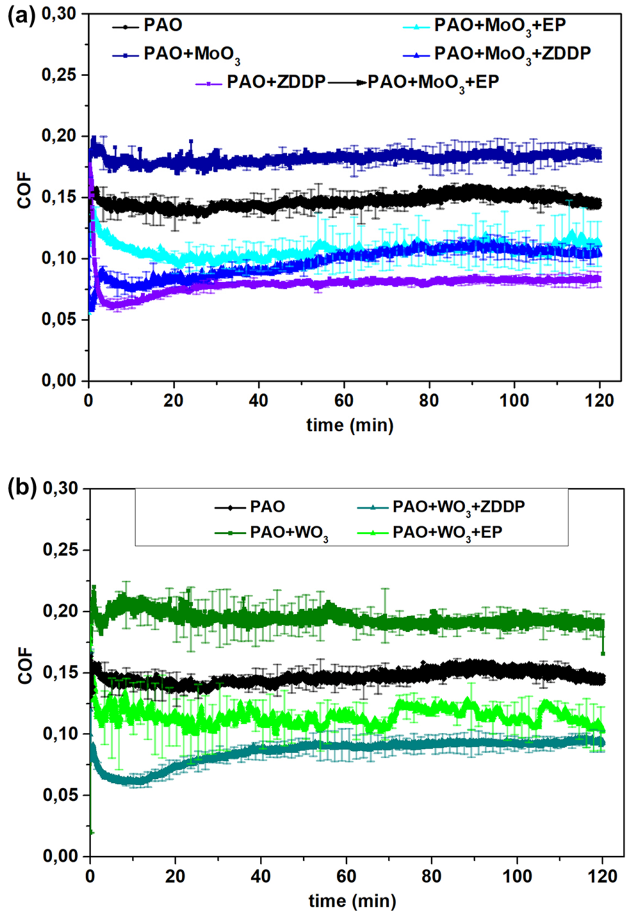


**Fig. 3** Coefficient of friction as a function of time for the lubricant mixtures containing **a** $MoO_3$ nanotubes and **b** $WO_3$ nanoparticles in combination with ZDDP and EP. The friction value obtained with pure PAO is shown as reference value in both cases

## 2.2 Lubricant Mixtures

The transition metal oxide nanoparticles were mixed in poly-alpha olefin 4 (PAO) base oil using a concentration of 5 wt%. In order to promote the formation of TMD tribofilms via the in-situ sulphurization of the TMO nanoparticles, two different Sulphur-containing additives widely used in lubricant formulations were selected: Zinc dialkyl dithiophosphate (ZDDP) anti-wear additive (AW), with a primary alkyl structure and 99% purity and sulphurized olefin polysulphide (40% of sulphur content) extreme pressure additive (EP). Both additives were provided by Lukoil Lubricants Europe (Austria) and were used with a concentration of 2 wt%. An ultrasonic processor VC 505 (Sonics & Materials. Inc, USA) was used for homogenizing the nanolubricant mixtures before the test. The selected parameters for the probe tip were 20% amplitude during 8 min, while the pulse was on and off for 2 s.

**Table 1** Summary of the test parameters

| Parameter | SRV test | Brugger test |
|---|---|---|
| Normal load (N) | 25 | 400 |
| Initial contact pressure (GPa) | 0.9 | 1.4 |
| Stroke (mm) | 1.5 | – |
| Frequency (Hz) | 25 Hz | – |
| Speed (m/s) | 0.04 (average) | 1.25 |
| Temperature (°C) | 40 | 23 |
| Test duration (s) | 7200 | 30 |

## 2.3 Tribological Experiments

The nanolubricants containing transition metal oxide nanoparticles were investigated under two different contact conditions (Table 1). A group of experiments was performed under reciprocating sliding conditions in order to investigate the friction performance of the mixtures as function of time and correlate the observed frictional behaviour with the tribochemical reactions occurring in the contact. A second set of experiments was performed using a Brugger test setup. The Brugger test imparts more severe contact conditions in terms of pressure and is particularly suitable for promoting the reaction of active additives such as extreme pressure but is less sensitive to adsorptive agents.

The tribological experiments were performed using a SRV® tribometer (Optimol Instruments Prüftechnik GmbH, Germany) under reciprocating sliding conditions with a ball-on-flat configuration. The selected discs were made of bearing steel (AISI 52100), characterized by a fine martensitic microstructure containing disperse micrometre size carbides. The balls were also made of bearing steel (AISI 52100) and had a diameter of 10 mm. Both the discs and the balls had a roughness of $R_a$ 0.05 µm and a hardness of 850 HV10. Prior to the tests, all samples were carefully cleaned in ultrasonic bath during 20 min (10 min with toluene and 10 min with petroleum ether). The reciprocating sliding experiments were performed at a constant normal load of 25 N, resulting in an average Hertzian contact pressure of 0.9 GPa. The stroke was set to 1.5 mm with a reciprocating sliding frequency of 25 Hz. Throughout the experiment, the temperature was kept constant at 40 °C. The test duration was one hour in order to ensure that steady-state conditions were achieved before the end of the experiment.

The Brugger tests according to DIN 51347-1 and 2 were performed using two AISI 52100 crossed cylinders. The test cylinder had a diameter of 8 mm with a roughness $R_a < 0.2$ µm and a hardness of 65 HRC, whereas the friction ring had a diameter of 25 mm with a roughness $R_a < 0.8$ and a hardness of 60 HRC. The test cylinder was placed with the axis perpendicular to the rotating friction ring, which was pressed at a constant normal load of 400 N against the test cylinder while rotating with a linear velocity of 1.25 m/s. This contact situation resulted in an elliptical contact are with a mean contact pressure of 1.4 GPa. After the experiments, the wear scar on the test cylinder was measured using light microscopy in order to determine the Brugger value. The Brugger value quantifies the load carrying capacity of the lubricant and is defined as the normal load divided by the area of the wear scar. Since the normal load is kept constant for all experiments, the smaller the wear scar, the better the load-carrying capacity of the investigated lubricants.

### 2.4 Surface and Tribochemical Analyses

The morphology of the wear scars after the tribological experiments tests was characterized using a scanning electron microscope (JEOL JSM 6500F, JEOL Ltd., Japan). The SEM was operated using secondary or backscattered electrons with an acceleration voltage of 20 kV. The elemental composition of selected regions of the wear scars were investigated using electron dispersive X-ray diffraction (EDX) in order to reveal tribofilm formation.

The chemical composition of the tribofilms was determined using X-ray photoelectron spectroscopy (XPS) using a Thermo Fisher Scientific Theta Probe equipped with a monochromatic Al K$\alpha$ X-ray source (h$\nu$ = 1486.6 eV) and Ar + ion gun. The base pressure inside the XPS chamber was kept constant at values in the range of $10^{-7}$ Pa during the measurements. Prior to the tests, the investigated samples were ultrasonically cleaned in toluene followed by petroleum ether (both HPLC grade) before the tests and subsequently sputtered in the XPS chamber using soft Ar + for 20 s, with 3 kV and 1 μA sputter current in order to remove the remaining contaminants. A pass energy of 50 eV was used for the high-resolution spectra and the resulting binding energies were referenced to adventitious carbon at a binding energy of 284.6 eV.

## 3 Results and Discussion

### 3.1 Frictional Behaviour of Transition Metal Oxides with Sulphur-Containing Additives

The frictional performance of the nanolubricants containing $MoO_3$ nanotubes and $WO_3$ nanoparticles is summarized in Fig. 3. The coefficient of friction of neat PAO leading to a constant value of 0.15 is given as reference. The results show that the straight use of transition metal oxide-based nanolubricants leads to a relatively high coefficient of friction with a value close to 0.2 for $WO_3$ nanoparticles and slightly below for $MoO_3$ nanotubes. The addition of ZDDP to the lubricant mixtures leads to a drastic friction improvement. The synergy between $MoO_3$ nanotubes with ZDDP results in a low coefficient of friction with an initial value of 0.06 that slightly rises throughout the duration of the experiment until achieving a value slightly below 0.10. This behaviour was well reproducible in all the test repetitions performed. In case of $WO_3$, friction has an initial value of 0.09 and sharply decreases during the initial 10 min of the experiment down to a value of 0.06. Afterwards, this values rises and stabilizes up to a final steady-state value of 0.09.

A similar improvement in friction is obtained when adding EP instead of ZDDP to the transition metal oxide nanolubricants. The combination of EP with $MoO_3$ nanotubes leads to a constant coefficient of friction of around 0.10, after a 20 min running-in period with a higher friction value. The final average coefficient of friction is identical when using $MoO_3$ nanotubes with ZDDP or with EP as accompanying additive. However, the higher standard deviation of the friction plot is a hint that highlights the more unsteady frictional values obtained with the lubricant mixture containing EP. For $WO_3$ nanoparticles, the coefficient of friction at the beginning of the experiment has a value of 0.17, which is followed by a sudden decrease after a few minutes down to a value around 0.11. In this latter case, the friction is also more erratic when compared with the experiments performed using ZDDP.

An interesting aspect is the interaction of $MoO_3$ nanotubes with EP additive in the presence of well-stablished ZDDP tribofilms. To this end, an experiment was run using a mixture of PAO with ZDDP (without nanotubes) during 2 h under the same experimental conditions. Afterwards, the remaining lubricant was gently removed and the test proceeded for two additional hours with a mixture containing $MoO_3$ and EP. The results show a drastic friction reduction from 0.17 down to 0.06 and a subsequent stabilization at a steady-state level of 0.07. Note also that this case resulted in the lowest standard deviation highlighting a higher reproducibility between identical tests. The friction levels reached are comparable to those attained using lubricant mixtures containing ZDDP and molybdenum dithiocarbamate (MoDTC) [30]. The main advantage of the presented approach is that it does not rely on organomolybdenum compounds for achieving low friction but on inorganic nanoparticles.

### 3.2 Morphology of the Wear Scars

The straight use of $MoO_3$ as lubricant additive leads to a wear scar morphology that indicates the presence of mild wear (Fig. 4a). At high magnifications (Fig. 4b), the presence of voids suggests the occurrence of corrosion during the experiment. Since the lubricant mixture contains uniquely hydrocarbon oil and $MoO_3$ nanotubes, the most plausible way to explain the observed wear mechanism is by formation of molybdic acid ($H_2MoO_4$) due to reaction of the nanotubes with moisture.

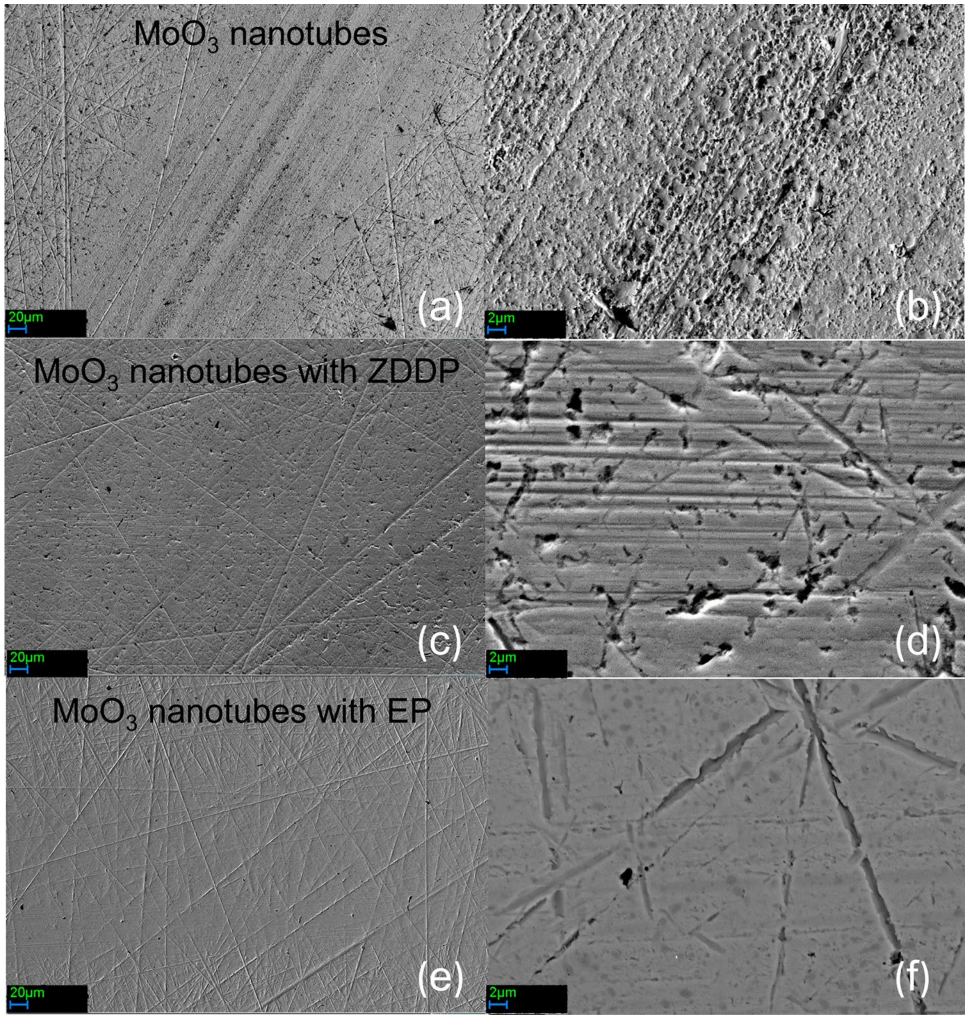


**Fig. 4** Surface topography after reciprocating sliding with the lubricant mixtures containing **a**, **b** $MoO_3$ nanotubes alone, **c**, **d** $MoO_3$ nanotubes with ZDDP and **e**, **f** $MoO_3$ nanotubes with EP

The use of $WO_3$ nanoparticles in PAO oil results in a remarkable wear protection. The original grinding lines present in the 100Cr6 disc are clearly visible throughout all the wear scar (Fig. 5a) and only higher magnifications allow observing some degree of plastic deformation in the grinding lines accompanied by the presence of very mild abrasion marks (Fig. 5b). The wear scar has in general a lighter colour, with regions showing the presence of a white colour tribofilm. These regions are W-rich, as suggested by the lighter colour due to the heavy atomic weight of W, and is verified by EDX analyses that reveal an atomic concentration of W of up to 20 at.% in contrast to the 2 at% detected in the other regions.

The wear track after the experiment using $MoO_3$ and ZDDP has a morphology characterized by very little signs of wear. Within the wear scar, the original grinding marks present due to sample preparation are still visible (Fig. 4c). At higher magnifications, subtle abrasive wear marks can be identified running parallel to the sliding direction in very localized regions of the wear scar. Minor signs of plastic deformation can also be seen at the edges of the grinding marks (Fig. 4d). The detection of Mo, Fe and O in the wear scar with sporadic spot measurements detecting Mo concentrations as high as 42 at.% suggests the possible presence of $MoO_3$ nanotubes remains over the Fe substrate. The outer edges of the wear scar show regions of darker colour with no hints of surface degradation. The presence of Zn (7.7 at.%) indicates the formation of a ZDDP tribofilm. The observed surface morphology highlights the superb performance of this nanolubricant mixture in terms of friction and wear and evidences that the excellent anti-wear properties of ZDDP are preserved, when used in conjunction with $MoO_3$ nanotubes. The anti-wear protection of ZDDP relies on the formation of a soft tribofilm containing Zn, P and S that is steadily formed and removed on the steel surface during the sliding process, thus acting as a sacrificial layer. These anti-wear mechanisms are usually accompanied by a high friction, thus making the use of friction modifiers unavoidable. As consequence, the low coefficient of friction measured for the mixture of $MoO_3$ nanotubes and ZDDP cannot be attributed uniquely to the formation of a ZDDP tribofilm.

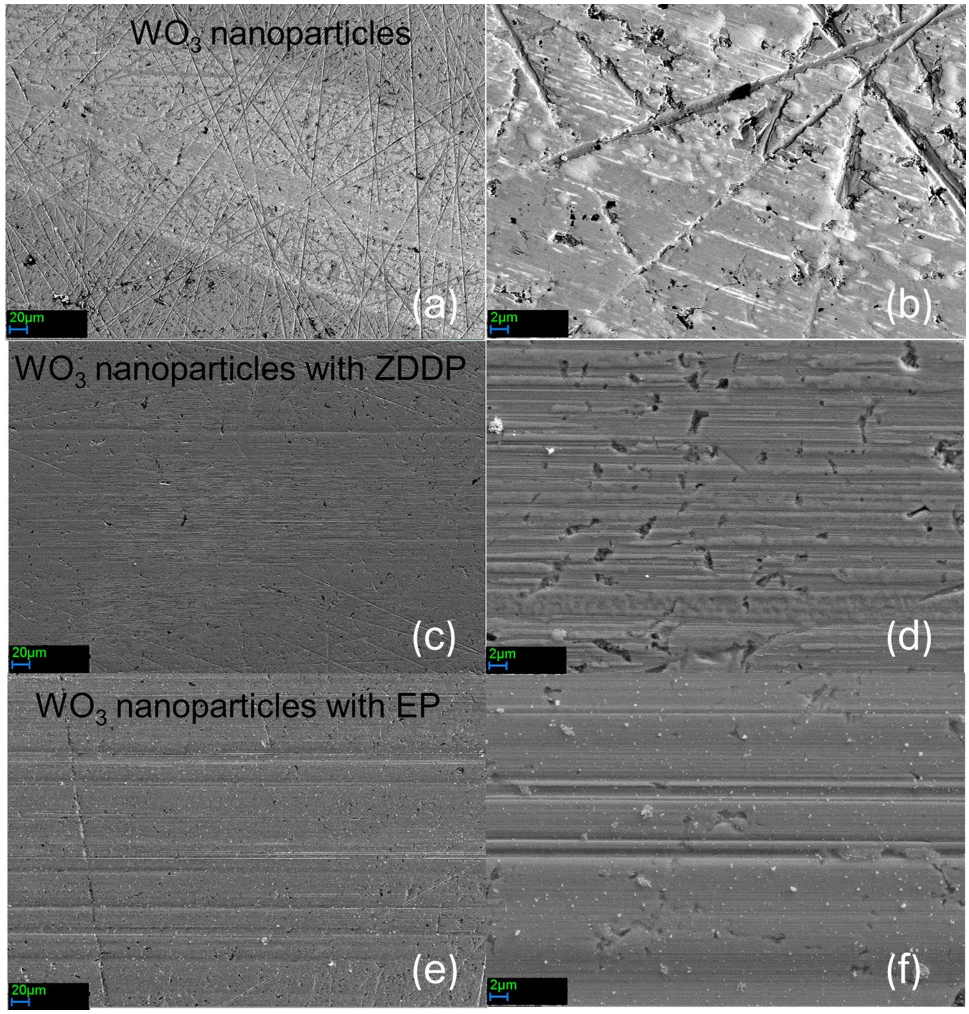


**Fig. 5** Surface topography after reciprocating sliding with the lubricant mixtures containing **a**, **b** $WO_3$ nanoparticles alone, **c**, **d** $WO_3$ nanoparticles with ZDDP and **e**, **f** $WO_3$ nanoparticles with EP

As similar wear scar morphology is observed when using the nanolubricant containing $WO_3$ and ZDDP. This mixture results in the formation of a dark-coloured tribofilm in the sliding region with a complete lack of wear (Fig. 5c). No signs of surface degradation can be noticed even at magnifications of 5000× (Fig. 5d). The elemental analyses of the tribofilm show the presence of W and O (up to 2.6 and 15.6 at.%, respectively), combined with Zn (3.8 at.%) in the dark patchy regions of the tribofilm.

The nanolubricant containing $MoO_3$ nanotubes and EP led to a surface morphology, characterized by a very mild wear. The original grinding marks present on the sample surface were slightly worn during the experiment but were still visible at its conclusion. At higher magnification, the grinding marks show some minor plastic deformation at the edges. The rest of the surface is somewhat smoothen, suggesting the occurrence of some minor tribochemical polishing effect. An EDX analysis of the tribofilms reveals the presence of 0.6 at.% of S. Even though no colour contrast can be observed in the wear scar under SEM, the presence of S indicates the potential formation of a $MoS_2$ tribofilm.

The combination of $WO_3$ nanoparticles with EP additive results in mild abrasive wear, as evidenced by the grinding marks oriented parallel to the sliding direction in the wear scar. At high magnification, some white spots can be observed that correspond to the presence of $WO_3$ nanoparticles.

### 3.3 Extreme Pressure Performance of Transition Metal Oxide Nanoparticles and Sulphur-Containing Additives Under Unidirectional Sliding

The performance of the transition metal oxide nanolubricants under unidirectional sliding contact in extreme pressure conditions is evaluated using the Brugger test. The results are expressed as a load carrying capacity number for each nanolubricant. The load carrying capacity (LCC) is calculated by dividing the normal load applied during the experiment by the resulting worn area. This means that a higher load carrying capacity implies a better wear protection under the imparted test conditions. The LCC for the pure PAO oil is 21, a poor value. As reference, the LCC for PAO containing 2 wt.% EP additive is 85, whereas a mixture of PAO and 2 wt.% ZDDP has a value of 29. This means that the Brugger test promotes the activation of EP additives and is particularly suitable for investigating the EP performance of lubricants. Having these reference values in mind, the results of all nanolubricants are shown in Fig. 6.

The nanolubricants containing $MoO_3$ nanotubes have a radically different behaviour depending on the accompanying sulphur-containing additive. When $MoO_3$ nanotubes are use straight in PAO, the LCC reaches a value of 24 N/mm$^2$, very close to the reference value obtained for pure PAO. This result clearly highlights that $MoO_3$ nanotubes do not provide any benefit as EP additives. The addition of ZDDP in combination with $MoO_3$ nanotubes results in a marginal, but statistically representative improvement in LCC up to 34 N/mm$^2$. This increase suggests the occurrence of a tribochemical reaction between ZDDP and the $MoO_3$ nanotubes. However, a more dramatic increase in LCC occurs when replacing ZDDP by EP as accompanying additive to the $MoO_3$ nanotubes. In this case, the LCC increases over a factor 6 up to a value of 156 N/mm$^2$ much higher than the LCC achieved using PAO with EP. A reference mixture containing PAO and $MoS_2$ nanotubes having an identical morphology reaches a value of 105 N/mm$^2$, slightly higher than PAO with EP, but lower than $MoO_3$ nanotubes with EP. As reported in a previous work of the authors [27], the reason for this extraordinary performance is attributed to the in-situ sulphurization of the $MoO_3$ nanotubes during the unidirectional sliding process. Conventional EP additives undergo under the same conditions a tribochemical reaction with the iron substrate that leads to the formation of iron sulphides. These iron sulphides formed on the surface prevent metal-to-metal contact between the rubbing crossed cylinders and lead to a massive decrease in wear, as indicated by a higher LCC. The tribochemical behaviour of $MoS_2$ nanotubes in extreme pressure conditions is somewhat analogous. Under lower contact pressures, $MoS_2$ nanotubes provide an excellent friction performance by exfoliating and building a $MoS_2$ tribofilm between the sliding counterbodies that enable easy glide. At higher pressures, as during the Brugger test, $MoS_2$ nanotubes start partly reacting with iron substrates building iron sulphides and molybdenum oxides. This process is still accompanied by exfoliation of $MoS_2$ platelets, which results in a complex tribofilm consisting in a combination of sulphides and oxides of both, molybdenum and iron. These tribofilms were originally observed in $WS_2$ nanoparticles by Ratoi et al. [18]. Our results suggest that this process may lead to a gradual consumption of the $MoS_2$ available in the base oil. On contrary, the use of $MoO_3$ nanotubes leads to the formation of similar tribofilms that have at least a certain degree of regeneration by the in-situ formation of $MoS_2$, as long as S from the EP additive is available. A similar observation was done by Dassenoy et al. when using $WS_2$ nanoparticles in combination with ZDDP [13]. In their case, the frictional performance of $WS_2$ nanoparticles at 100 °C during reciprocating sliding decreased due to the formation of $WO_3$ during rubbing. However, in combination with ZDDP, friction remained low, while XPS analyses showed the presence of $WS_2$ in the tribofilm. This behaviour was attributed to oxidation protection by the ZDDP additive, but the present work seems to indicate that in-situ re-sulphurization of the tribofilm may have occurred at that time too.

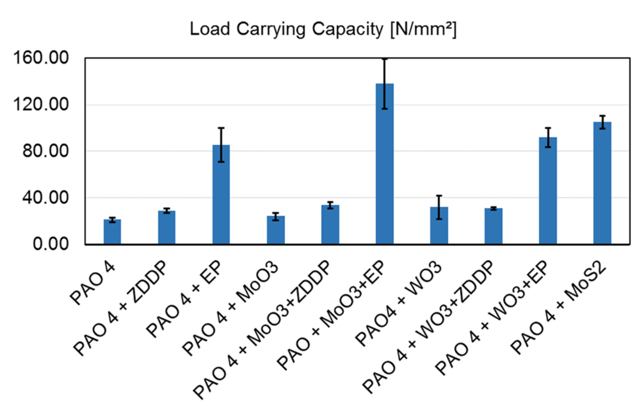


**Fig. 6** Load-carrying capacity of the lubricant mixtures during Brugger tests

The use of $WO_3$ nanoparticles in the nanolubricants resulted in a different behaviour compared to $MoO_3$ nanotubes, which also depended on the accompanying sulphur additive. $WO_3$ nanoparticles alone were able to improve the LCC of PAO up to 32 N/mm$^2$, indicating that $WO_3$ nanoparticles have the capacity to create wear-resistant tribofilms. A similar LCC (31 N/mm$^2$) was obtained when using $WO_3$ nanoparticles in combination with ZDDP albeit with a smaller standard deviation. This result suggests that the wear protection is provided by the $WO_3$ nanoparticles and that ZDDP has a very little role in the process, if any. When adding EP, $WO_3$ nanoparticles led to a LCC value of 91 N/mm$^2$, very close to the LCC achieved by the EP additive alone.

The surface morphology of the wear scars after the Brugger tests was analysed using SEM/EDX (Figs. 7, 8 and 9). The use of $MoO_3$ nanotubes without any sulphur-containing additive results in a large wear scar (Fig. 8a, b). The morphology of the wear scar shows the presence of pits as consequence of adhesive wear with torn metal as consequence of severe plastic deformation. Some grinding marks can be observed running in sliding direction as a consequence of abrasion. The EDX analyses show the presence of Mo with content ranging from 0.5 to 2 wt.%, depending on the spot position. The addition of ZDDP to the $MoO_3$ nanotubes results in a wear scar with slightly smaller dimension (Fig. 8c, d). Within the wear scar, the regions of adhesion and severely sheared metal are combined with very smooth

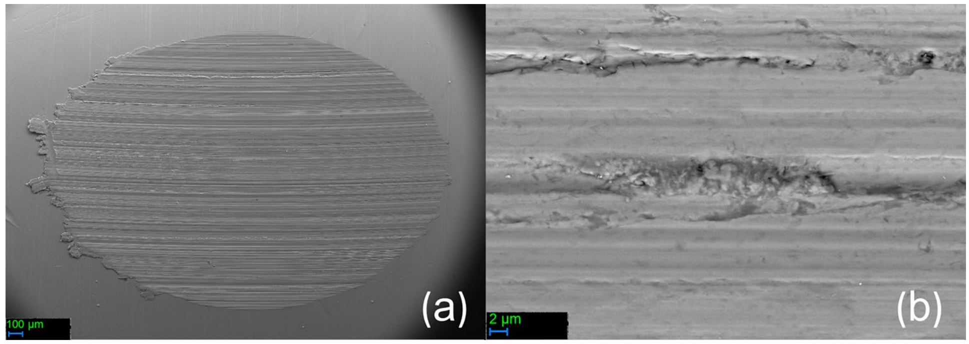


**Fig. 7** Surface topography after the Brugger test for a reference lubricant mixture containing PAO base oil and EP additive, without nanoparticles

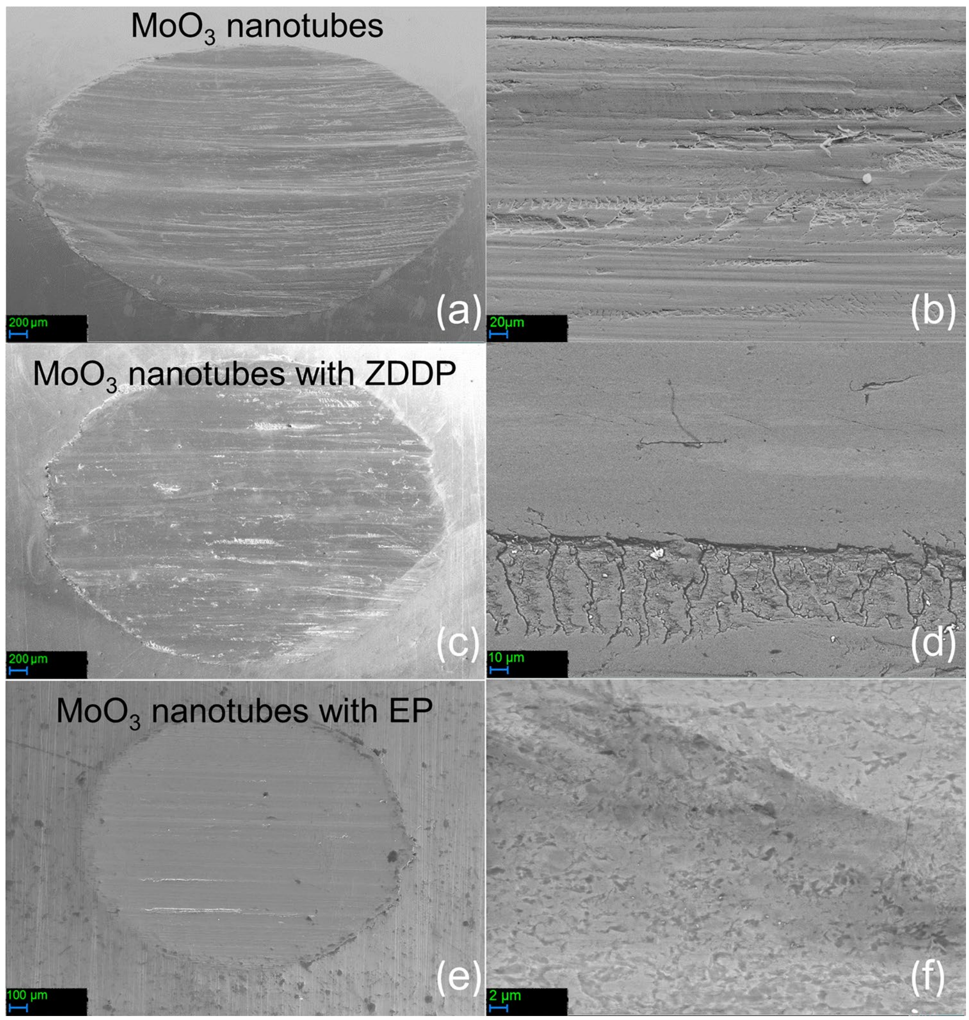


**Fig. 8** Surface topography after the Brugger test for the lubricant mixtures containing $MoO_3$ nanotubes alone (**a**, **b**), $MoO_3$ nanotubes with ZDDP (**c**, **d**) and $MoO_3$ nanotubes with EP (**e**, **f**)

regions with a lower degree of adhesive wear. The smooth regions contain wider smear regions, which are Mo-rich (3.3 at.%) and suggest tribofilm formation. On contrary, no presence of Zn could be detected using EDX. Finally, the combination of $MoO_3$ nanotubes with EP additive leads to the smallest wear scar, and as consequence, to the highest LCC, as mentioned above (Fig. 8e). Besides its extraordinary small size, the wear scar is extremely smooth, even when amplified up to 5000×, without any signs of adhesive wear (Fig. 8f). The elemental composition analysis reveals the presence of Mo (up to 3.2 at.%) and S (up to 5.6 at.%) suggesting the formation of a Mo-rich tribofilm.

The use of $WO_3$ nanoparticles as lubricant additive in the Brugger test results in the formation of a wear scar slightly smaller when compared to pure PAO. The reason for the improvement seems to lie in the formation of a thin $WO_3$ tribofilm. As seen in Fig. 9a, smeared W-rich

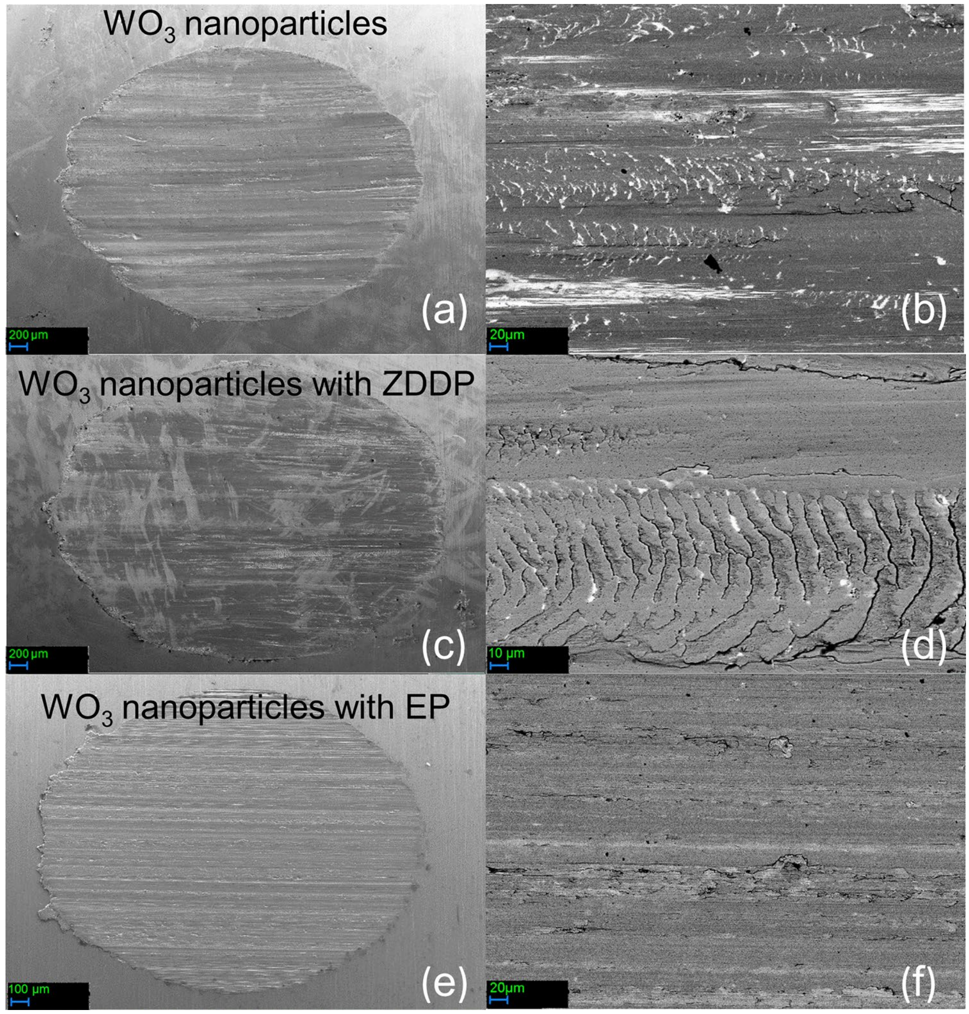


**Fig. 9** Surface topography after the Brugger test for the lubricant mixtures containing $WO_3$ nanoparticles alone (**a**, **b**), $WO_3$ nanoparticles with ZDDP (**c**, **d**) and $WO_3$ nanoparticles with EP (**e**, **f**)

patches can be easily identified within the wear scar thanks to the high contrast given by the large atomic number of W (Fig. 9b). In other locations of the wear scar, $WO_3$ nanoparticles can be identified agglomerated in regions with highly sheared metal. The combination of $WO_3$ nanoparticles with ZDDP results in a wear scar with similar dimensions but with a different morphology (Fig. 9c). In this case, $WO_3$ nanoparticles are found smash either individually or in small agglomerates, but no tribofilm formation could be observed (Fig. 9d). Also in this case, no Zn signal could be detected by EDX. The use of $WO_3$ nanoparticles combined with EP additive results in a significant decrease in the wear scar dimensions (Fig. 9e). The underlying reasons for this decrease are hinted by the morphology at higher magnifications. In this case, the wear does not show any evidence of adhesive wear and the EDX analyses reveal the formation of a S-rich tribofilm (2.4 at.%) (Fig. 9f). The presence of W is not visible, despite its high contrast under SEM. However, traces of W (up to 1.8 at.%) can be measured according to EDX.

### 3.4 Tribochemical Interaction Between Metal Oxide Nanoparticles and Sulphur-Containing Additives

The chemical composition of the resulting tribofilms after the experiments was investigated using XPS for the reciprocating sliding SRV experiments and for the unidirectional sliding Brugger tests (Fig. 10). For the SRV experiments, the nanolubricant containing $MoO_3$ nanotubes with ZDDP built a characteristic ZDDP tribofilm formed by Zn and P in form of ZnS, ZnO and phosphates. Besides the ZDDP tribofilm, the tribochemical formation of $MoS_2$ was evidenced by the presence of a peak at 228.1 eV. This results are in agreement with Raman spectroscopy analyses performed by the authors on identical tribofilms, and that reveals the presence of peaks at 377 and 403 $cm^{-1}$ [27]. The combination of $MoO_3$ nanotubes with EP additive resulted in the formation of a tribofilm formed by molybdenum oxides (binding energy of 231.5), molybdenum disulphide (binding energy 228.9), iron sulphide and iron oxides. This means that during sliding contact, the

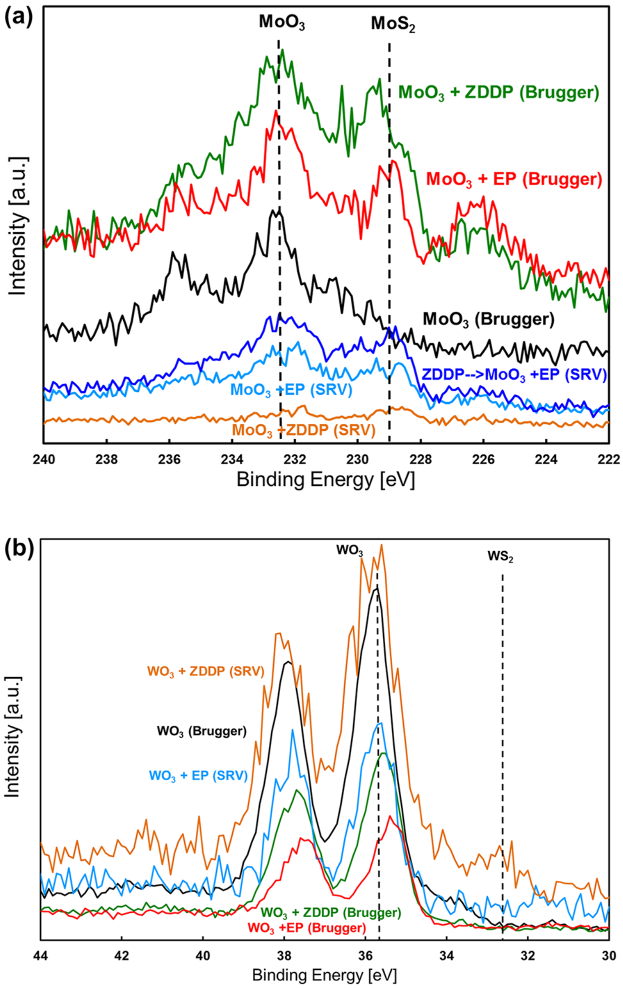


**Fig. 10** High-resolution XPS spectra for the experiments performed under reciprocating sliding and the Brugger tests using different lubricant mixtures containing $MoO_3$ nanotubes (**a**) and $WO_3$ nanoparticles (**b**)

sulphurized olefin reacts with both the $MoO_3$ nanotubes and the steel substrate. The simultaneous formation of iron and molybdenum oxides and sulphides resulted in an anti-wear performance slightly worse than when having a protective ZDDP tribofilm together with $MoO_3$ nanotubes, but in a similar friction level. It was noted in a previous paper of the authors that the presence of EP degrades the frictional performance of $MoS_2$ nanotubes [15]. On contrary, $MoS_2$ tribofilms are able to maintain a coefficient of friction around 0.07 in the presence of ZDDP tribofilms, even at 40 °C, provided that they are well formed [9].

In the case of $WO_3$ nanoparticles, their combination with ZDDP resulted in the formation of a similar ZDDP tribofilm, as highlighted by the presence of ZnO, ZnS and phosphates. However, in this case, W was found to be as oxide, with a peak at 35.2 eV. Also in the case of $WO_3$ nanoparticles combined with EP, no formation of $WS_2$ could be found. In the latter, the only sulphide formed can be attributed to iron sulphide. Iron oxides were also present in the wear scar.

The tribofilms formed during the Brugger test using $MoO_3$ nanotubes are characterized as expected by the presence of $MoO_3$ and iron oxides. This spectrum is particularly useful as reference. The addition of ZDDP results in the formation of $MoS_2$, accompanied by the presence of Zn and P in the form of ZnS, ZnO and phosphates. The latter indicated the presence of a ZDDP tribofilm. In the case of using $MoO_3$ nanotubes with EP additive, the tribofilm formed is formed by a combination of molybdenum and iron sulphides and oxides, similar to the one formed under reciprocating sliding conditions but with a higher sulphide content. This indicates that $MoO_3$ partly sulphurizes in the presence of EP additives, building in-situ a $MoS_2$ tribofilm. The load-carrying capacity measured indicates that the latter offers a better lubricity probably due to the continuous formation of $MoS_2$ during the sliding process, as a consequence of the presence of S. A similar effect was reported by Aldana et al. when using IF-$WS_2$ nanoparticles at 100 °C under reciprocating sliding [13]. The authors found a higher sulphide-to-oxide ratio when using $WS_2$ nanoparticles with ZDDP when compared to nanoparticles alone. This observation was justified by the known antioxidant properties of ZDDP but the in-situ re-sulphurization of oxidized nanoparticles or oxidized tribofilm as reported in the present work may have also contributed to their observations.

The straight use of $WO_3$ nanoparticles led to the formation of a tribofilm containing $WO_3$ and iron oxides. The addition of ZDDP did not change the chemical composition of the tribofilm. The lack of Zn and P indicated that the nanolubricant was not able to build a ZDDP tribofilm under these conditions. The mixture containing $WO_3$ nanoparticles and EP additive formed a tribofilm composed by iron sulphides and iron oxides. The presence of $WO_3$ was also evidenced but with a lower concentration, when compared to the mixtures having $WO_3$ nanoparticles and $WO_3$ nanoparticles with ZDDP, as already anticipated by the SEM images. The chemical composition of this tribofilm justifies the LCC measured for this mixture. The value obtained was very similar to the LCC measured for PAO with EP, suggesting a similar wear protecting mechanisms based on the formation of iron sulphides. The marginal improvement may be due to the additional protection provided by $WO_3$, even though both values are quite close to assure this statement without further research.

The XPS analyses show that $MoO_3$ nanotubes have a higher reactivity with S-containing additives compared to $WO_3$. While these results are in agreement with the observations performed during the Brugger tests, the reciprocating sliding experiments showed a very clear and significant friction reduction when $WO_3$ was accompanied by a sulphur-containing additive. For this reason, the reciprocating

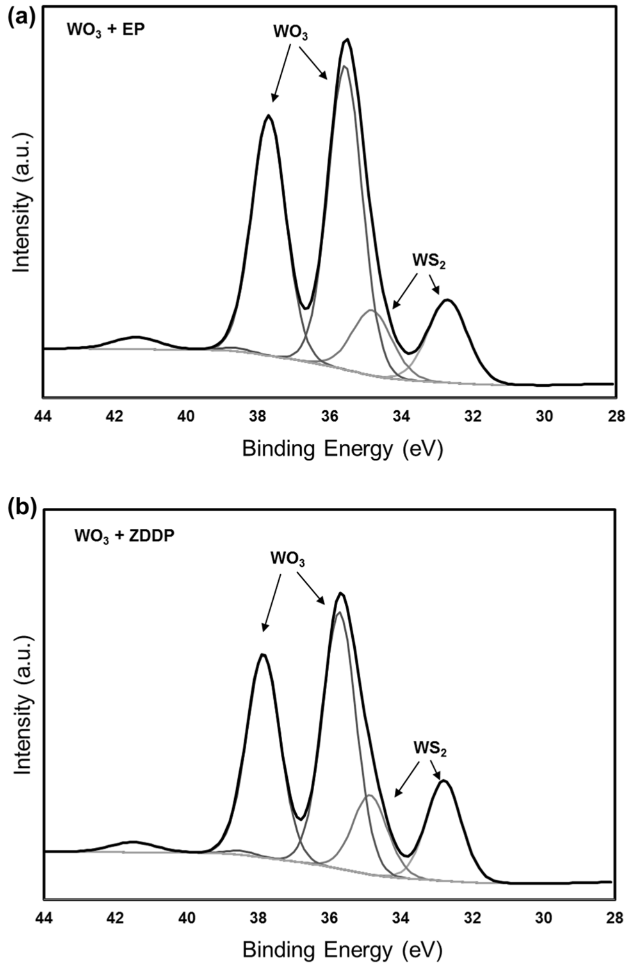


**Fig. 11** High-resolution XPS spectra of W 3d acquired from reciprocating sliding tests interrupted after 10 min using $WO_3$ nanoparticles with ZDDP (**a**) and WO3 (**b**) nanoparticles with EP as lubricants

sliding experiments using $WO_3$ with ZDDP and EP additive were repeated and interrupted after 20 min. This running-in time was selected based on the friction curves shown in Fig. 3, since they correspond to the minimum friction value achieved by the lubricant mixture of $WO_3$ and ZDDP.

XPS analyses of the interrupted test show a completely different chemical composition (Fig. 11) In this case, either the combination of $WO_3$ nanoparticles with ZDDP or EP leads to the formation of a clear $WS_2$ peak. These results justify the friction curves and indicate that the initially formed $WS_2$ progressively oxidizes during the duration of the experiment to $WO_3$. In general, it has been observed that $MoO_3$ are more prone to form $MoS_2$ tribofilms compared to $WO_3$. In a recent work by some of the authors [31], we showed that the in-situ formation of transition metal dichalcogenides tribofilms by a tribochemical reaction with Mo and W substrates relies first on the oxidation of the substrates to $MoO_3$ and $WO_3$, respectively, and that these compounds are those ultimately leading to $MoS_2$ and $WS_2$. In this work, we also noted that the formation of TMD tribofilms can be more easily achieved with Mo compared to W substrates, as observed in the present study.

## 4 Conclusions

The present work has shown the feasibility of using transition metal oxide nanoparticles for the in-situ formation of $MoS_2$ and $WS_2$ tribofilms. These tribofilms are tribochemically formed during reciprocating sliding using either $MoO_3$ nanotubes or $WO_3$ nanoparticles. In the case of $MoO_3$ nanotubes, $MoS_2$ was measured on all tribofilms, independently of the accompanying S additive and the contact conditions. On the contrary, $WS_2$ could only be detected during the initial states of reciprocating sliding.

The friction levels achieved by these tribofilms can be as low as 0.06 in case of $MoO_3$, provided that a well-stablished ZDDP tribofilm is formed. In the case of $WO_3$, the combination with ZDDP leads to a similar value during the beginning of the experiment as consequence of the formation of $WS_2$, followed by an increase due to the oxidation of the tribofilm to $WO_3$. Under mild reciprocating sliding conditions, it was also shown that $WO_3$ nanoparticles alone are able to provide a certain degree of anti-wear properties but accompanied by a high friction.

Under extreme pressure conditions, the combination of EP additives and $MoO_3$ nanotubes results in a load-carrying capacity able to outperform either EP additive or $MoS_2$ nanotubes. The reason is attributed to a continuous re-sulphurization of the tribofilm during the experiment. While $MoS_2$ nanotubes build $MoO_3$ during sliding, the presence of S in the lubricant allows for a continuous re-sulphurization of $MoO_3$ throughout the experiment, providing a higher load-carrying capacity. This re-sulphurization mechanism is likely to be the same as observed for TMD nanoparticles in the presence of S-containing additives, such as ZDDP.

**Acknowledgements** This work was funded by the Austrian COMET Programme (Project K2 XTribology. No. 849109) and carried out at the "Excellence Centre of Tribology". This project has also received funding from the European Union's Horizon 2020 research and innovation programme under the Marie Skłodowska-Curie Grant Agreement No 665778. The author A. Tomala acknowledges the POLONEZ Project by National Science Centre, Poland under fellowship registration number 2015/19/P/ST8/02597. The authors would like to acknowledge Dr. C. Gabler and Dr. C. Tomastik for performing the XPS measurements.

## References

1. Gibney, E.: 2D or not 2D? Nature **522**, 274–276 (2015)

2. Rapoport, L., Bilik, Y., Feldman, Y., Homyonfer, M., Cohen, S.R., Tenne, R.: Hollow nanoparticles of WS2 as potential solid-state lubricants. Nature **387**, 791–793 (1997)
3. Tenne, R., Margulis, L., Genut, M., Hodes, G.: Polyhedral and cylindrical structures of tungsten disulphide. Nature **360**, 444–446 (1992)
4. Margulis, L., Salitra, G., Tenne, R., Talianker, M.: Nested fullerene-like structures. Nature **365**, 113–114 (1993)
5. Remškar, M., Škraba, Z., Regula, M., Ballif, C., Sanjinés, R., Lévy, F.: New crystal structures of WS2: microtubes, ribbons, and ropes. Adv. Mater. **10**, 246–249 (1998)
6. Tannous, J., Dassenoy, F., Lahouij, I., Le Mogne, T., Vacher, B., Bruhács, A., Tremel, W.: Understanding the tribochemical mechanisms of IF-MoS 2 nanoparticles under boundary lubrication. Tribol. Lett. **41**, 55–64 (2011)
7. Kalin, M., Kogovšek, J., Remškar, M.: Nanoparticles as novel lubricating additives in a green, physically based lubrication technology for DLC coatings. Wear **303**, 480–485 (2013)
8. Niste, V.B., Ratoi, M.: Tungsten dichalcogenide lubricant nanoadditives for demanding applications. Mater. Today Commun. **8**, 1–11 (2016)
9. Tomala, A., Vengudusamy, B., Rodríguez Ripoll, M., Naveira Suarez, A., Remškar, M., Rosentsveig, R.: Interaction between selected MoS2 nanoparticles and ZDDP tribofilms. Tribol. Lett. **59**, 1–18 (2015)
10. Chen, Z., Liu, X., Liu, Y., Gunsel, S., Luo, J.: Ultrathin MoS2 nanosheets with superior extreme pressure property as boundary lubricants. Sci. Rep. **5**, 12869 (2015)
11. Joly-Pottuz, L., Dassenoy, F., Belin, M., Vacher, B., Martin, J.M., Fleischer, N.: Ultralow-friction and wear properties of IF-WS2 under boundary lubrication. Tribol. Lett. **18**, 477–485 (2005)
12. Jelenc, J., Remskar, M.: Friction on a single MoS2 nanotube. Nanoscale Res. Lett. **7**, 208 (2012)
13. Aldana, P.U., Vacher, B., Le Mogne, T., Belin, M., Thiebaut, B., Dassenoy, F.: Action mechanism of WS2 nanoparticles with ZDDP additive in boundary lubrication regime. Tribol. Lett. **56**, 249–258 (2014)
14. Aldana, P.U., Dassenoy, F., Vacher, B., Le Mogne, T., Thiebaut, B.: WS2 nanoparticles anti-wear and friction reducing properties on rough surfaces in the presence of ZDDP additive. Tribol. Int. **102**, 213–221 (2016)
15. Tomala, A., Rodríguez Ripoll, M., Gabler, C., Remškar, M., Kalin, M.: Interactions between MoS2 nanotubes and conventional additives in model oils. Tribol. Int. **110**, 140–150 (2017)
16. Tomala, A., Rodríguez Ripoll, M., Kogovšek, J., Kalin, M., Bednarska, A., Michalczewski, R., Szczerek, M.: Synergisms and antagonisms between MoS2 nanotubes and representative oil additives under various contact conditions. Tribol. Int. **129**, 137–150 (2019)
17. Rabaso, P., Dassenoy, F., Ville, F., Diaby, M., Vacher, B., Le Mogne, T., Belin, M., Cavoret, J.: An investigation on the reduced ability of IF-MoS2 nanoparticles to reduce friction and wear in the presence of dispersants. Tribol. Lett. **55**, 503–516 (2014)
18. Ratoi, M., Niste, V.B., Walker, J., Zekonyte, J.: Mechanism of action of WS2 lubricant nanoadditives in high-pressure contacts. Tribol. Lett. **52**, 81–91 (2013)
19. Orofeo, C.M., Suzuki, S., Sekine, Y., Hibino, H.: Scalable synthesis of layer-controlled WS2 and MoS2 sheets by sulfurization of thin metal films. Appl. Phys. Lett. **105**, 083112 (2014)
20. Morrish, R., Haak, T., Wolden, C.A.: Low-Temperature synthesis of n-type WS 2 thin films via $H_2S$ plasma sulfurization of $WO_3$. Chem. Mater. **26**, 3986–3992 (2014)
21. Kong, D., Wang, H., Cha, J.J., Pasta, M., Koski, K.J., Yao, J., Cui, Y.: Synthesis of MoS2 and MoSe2 films with vertically aligned layers. Nano Lett. **13**, 1341–1347 (2013)
22. He, Z., Que, W.: Molybdenum disulfide nanomaterials: structures, properties, synthesis and recent progress on hydrogen evolution reaction. Appl. Mater. Today. **3**, 23–56 (2016)
23. Remškar, M., Viršek, M., Mrzel, A.: The MoS2 nanotube hybrids. Appl. Phys. Lett. **95**, 2–4 (2009)
24. Leonard-Deepak, F., Castro-Guerrero, C.F., Mejía-Rosales, S., José-Yacamán, M.: Structural transformation of tungsten oxide nanourchins into IF–WS2 nanoparticles: an aberration corrected STEM study. Nanoscale **3**, 5076 (2011)
25. Kalin, M.: Influence of flash temperatures on the tribological behaviour in low-speed sliding: a review. Mater. Sci. Eng. A **374**, 390–397 (2004)
26. Ratoi, M., Niste, V.B., Zekonyte, J.: WS2 nanoparticles—potential replacement for ZDDP and friction modifier additives. RSC Adv. **4**, 21238 (2014)
27. Rodríguez Ripoll, M., Tomala, A., Gabler, C., Dražić, G., Pirker, L., Remškar, M.: In situ tribochemical sulfurization of molybdenum oxide nanotubes. Nanoscale. **10**, 3281–3290 (2018)
28. Remskar, M., Mrzel, A., Virsek, M., Godec, M., Krause, M., Kolitsch, A., Singh, A., Seabaugh, A.: The MoS2 nanotubes with defect-controlled electric properties. Nanoscale Res. Lett. **6**, 26 (2010)
29. Varlec, A., Arčon, D., Škapin, S.D., Remškar, M.: Oxygen deficiency in MoO3 polycrystalline nanowires and nanotubes. Mater. Chem. Phys. **170**, 154–161 (2016)
30. Morina, A., Neville, A., Priest, M., Green, J.H.: ZDDP and MoDTC interactions in boundary lubrication—the effect of temperature and ZDDP/MoDTC ratio. Tribol. Int. **39**, 1545–1557 (2006)
31. Kohlhauser, B., Rodríguez Ripoll, M., Riedl, Koller, C.M., Koutna, N., Amsüss, A., Hutter, H., Ramirez, G., Gachot, C., Erdemir, A., Mayrhofer, P.H.: How to get noWear? – A new take on the design of in-situ formed high performing low-friction tribofilms. Mater. Des. (2020) (in press)